

Asymptotically perfect efficient quantum state transfer across uniform chains with two impurities

Xining Chen, Robert Merea, and David L. Feder*

*Institute for Quantum Science and Technology, Department of Physics and Astronomy,
University of Calgary, Calgary, Alberta, Canada T2N 1N4*

(Dated: November 3, 2015)

The ability to transfer quantum information from one location to another with high fidelity is of central importance to quantum information science. Unfortunately for the simplest system of a uniform chain (a spin chain or a particle in a one-dimensional lattice), the state transfer time grows exponentially in the chain length N at fixed fidelity. In this work we show that the addition of an impurity near each endpoint, coupled to the uniform chain with strength w , is sufficient to ensure efficient and high-fidelity state transfer. An eigenstate localized in the vicinity of the impurity can be tuned into resonance with chain extended states by tuning $w(N) \propto N^{1/2}$; the resulting avoided crossing yields resonant eigenstates with large amplitudes on the chain endpoints and approximately equidistant eigenvalues. The state transfer time scales as $t \propto N^{3/2}$ and its fidelity F approaches unity in the thermodynamic limit $N \rightarrow \infty$; the error scales as $1 - F \propto N^{-1}$. Thus, with the addition of two impurities, asymptotically perfect state transfer with a uniform chain is possible even in the absence of external control.

I. INTRODUCTION

The ability to transfer information is crucial for digital communications. Likewise in quantum computation and communication, the ability to efficiently and reliably transfer quantum information is central to both current and future quantum technologies [1]. In the standard circuit model of quantum computation, the quantum information is encoded on localized spins with two or more accessible distinguishable quantum states (qubits or qudits), and an algorithm is effected by manipulating individual spins, performing two-spin operations, and making measurements [2]. The physical objects encoding the spins, for example spins in semiconductors [3] or nitrogen-vacancy centers in diamond [4], may be widely separated, requiring the development of robust quantum state transfer protocols for spin networks [5].

Schemes for perfect quantum state transfer (PST) in spin networks were developed over a decade ago [6, 7]. Quantum information encoded on a spin at one end of a linear chain of nearest-neighbor coupled spins was found to propagate perfectly to the opposite end, as long as the non-uniform spin coupling coefficients could be carefully chosen. Subsequent work showed how to find all possible coupling constants consistent with PST for a spin chain of arbitrary length [8, 9]. The ability to adjust a large number of coupling constants is expected to be experimentally challenging, and unfortunately PST is not possible in uniform spin chains (i.e. where all coupling constants are identical) longer than three sites. This has prompted the investigation of different network topologies with uniform (but possibly signed) couplings that can support PST [10–20].

An alternative strategy is to relax the assumption of

perfect quantum state transfer, replacing it with ‘pretty good state transfer’ (PGST) [21, 22] or equivalently ‘almost perfect state transfer’ (APST) [23]. In these cases, one sets the desired fidelity F of the output state, and determines the time required (if any) to achieve it. While these equivalent concepts in the literature are frequently referred to as APST, we prefer to employ the term ‘imperfect quantum state transfer’ (IST) to clearly distinguish the behavior from PST. In IST there exists a time at which the initial state at some site transfers to a different site with probability approaching unity to within some error.

For uniform spin chains, IST is only possible in principle for particular values of the number of spins N [22, 24]. For fixed minimum fidelity, however, the transfer time t increases exponentially with N [24]. A linear scaling of t with N can be achieved by coupling the initial and final spins only weakly to the uniform chains [25–34]. Because the quantum information is strongly localized in the vicinity of the chain ends at all times, this model is also more robust against noise than the bare uniform chain. Unfortunately, in this model after optimizing the strength of the weak coupling parameter (which is found to decrease like $N^{-1/6}$) and initializing the channel, the maximum output amplitude decreases with N , attaining an asymptotic value of 0.8469 for $N \rightarrow \infty$ [28]. Adding additional weak links improves the results, but the asymptotic error in fidelity remains finite [30]. Instead applying a magnetic field in the vicinity of the chain ends yields fidelities that approach unity in the large- N limit, but at the cost of t growing exponentially with N [33, 35–38].

In this work we consider a uniform spin chain of length N , with sites labeled from 1 through N , with the minor modification of an additional impurity spin coupling to the spin at site 3 and another to site $N - 2$, both with coupling constant w . The value of w is left as a variable to be optimized. It is found that there exists a value of

*Corresponding author: dfeder@ucalgary.ca

$w \sim \sqrt{N}$ that yields a resonance between the quantum state localized near the impurity and extended states of the chain. The resulting avoided crossing yields strongly mixed eigenvectors with equally spaced eigenvalues and large overlaps with the chain endpoints. Under these conditions, the fidelity for quantum state transfer from site 1 to site N approaches unity in the thermodynamic (large- N) limit, with error $1 - F \propto N^{-1}$. The system therefore exhibits ‘asymptotically perfect quantum state transfer,’ a behavior previously unobserved for a spin network. The time is also found to scale efficiently with the chain length, $t_{\text{IST}} \propto N^{3/2}$. In concrete terms, the output fidelity surpasses $F = 0.9$ when $N > 99$ and exceeds $F = 0.99$ for $N \geq 900$.

Section II briefly reviews the essential characteristics of IST, with an emphasis on mirror-symmetric networks such as spin chains. The model of interest in the present work is introduced in Sec. III. The minimum IST time found by optimizing the impurity coupling strength w is found to be a strongly non-monotonic function of N . To find a functional form for $w(N)$, the model is investigated analytically in Sec. IV; high-fidelity IST in time $t_{\text{IST}} \propto N^{3/2}$ is found to occur if $w(N) \propto \sqrt{N}$. Section V is devoted to a full numerical simulation of the evolution under the model Hamiltonian, validating and clarifying the analytical predictions. A brief discussion of the results is found in Sec. VI.

II. IMPERFECT QUANTUM STATE TRANSFER

The time evolution of a quantum state $|\phi(t)\rangle$ under the action of a governing Hamiltonian H is given by

$$|\phi(t)\rangle = e^{-itH/\hbar}|\phi(0)\rangle. \quad (1)$$

Suppose that $|\phi(t)\rangle$ is only defined at discrete sites $j = 1, 2, \dots, N$. Defining states $|i\rangle$ corresponding to unit basis vectors associated with site i , one obtains the probability amplitudes $\langle i|\phi(t)\rangle = \phi_i(t)$. Given N eigenvalues $\lambda^{(n)}$ and orthonormal eigenvectors $|\psi^{(n)}\rangle$ of H , Eq. (1) becomes

$$|\phi(t)\rangle = \sum_{n=1}^N \exp\left[-\frac{it\lambda^{(n)}}{\hbar}\right] |\psi^{(n)}\rangle \langle \psi^{(n)}|\phi(0)\rangle. \quad (2)$$

Suppose furthermore that the initial state is completely localized at a particular site j , so that $\langle i|\phi(0)\rangle = \delta_{ij}$. Eq. (2) can then be rewritten as

$$|\phi(t)\rangle = e^{-i\lambda^{(m)}t/\hbar} \sum_{n=1}^N e^{-it(\lambda^{(n)} - \lambda^{(m)})/\hbar} |\psi^{(n)}\rangle \langle \psi^{(n)}|j\rangle. \quad (3)$$

Evidently if $(\lambda^{(n)} - \lambda^{(m)})t/\hbar = 2\pi s$ ($s \in \mathbb{Z}$) for any n and m , then $|\phi(t)\rangle = |j\rangle$ for all j up to an unimportant overall phase; that is, the discrete Hamiltonian is site periodic. This immediately implies that the Hamiltonian

is site periodic if all the eigenvalues of H satisfy the ratio condition

$$\frac{\lambda^{(n)} - \lambda^{(m)}}{\lambda^{(p)} - \lambda^{(q)}} \in \mathbb{Q}, \quad (4)$$

for all possible indices $\{n, m, p, q\}$ (except $\lambda^{(p)} = \lambda^{(q)}$). For large systems in practice, condition (4) can only be satisfied if the spectrum is linear, i.e. the gap between successive non-degenerate eigenvalues is constant.

In perfect quantum state transfer (PST) between sites i and j , a state initially localized in state $|i\rangle$ ends up in state $|j\rangle$, $j \neq i$ (and vice versa) after some elapsed time t ; these sites are therefore periodic in time $2t$. PST therefore implies site periodicity, but the converse is not generally true. For space-symmetric Hamiltonians that commute with the parity operator, however, site periodicity implies PST. Suppose that the smallest difference in eigenvalues is $\Delta = \lambda^{(n)} - \lambda^{(m)}$ for some m and n ; then site periodicity occurs in time $t_P = 2\pi\hbar/\Delta$. Consider an initial state in a superposition state of sites i and j equidistant from an axis of symmetry, $|\phi(0)\rangle = \frac{1}{\sqrt{2}}(|i\rangle + |j\rangle)$. Because $|\phi(0)\rangle$ has even parity, only even-parity eigenvectors will contribute to the sum in Eq. (3). Site periodicity must be maintained, but the absence of odd eigenvalues implies that the gap has now doubled to $\Delta' = 2\Delta$ (assuming the spectrum is linear); now $t_P = 4\pi\hbar/\Delta'$. At half this time $t = t_P/2 = 2\pi\hbar/\Delta'$ the sum over n in Eq. (3) still resolves to the identity. Thus, even-parity states such as the superposition state $\frac{1}{\sqrt{2}}(|i\rangle + |j\rangle)$ evolve to themselves in half the site periodicity time $t = \pi\hbar/\Delta$, which is only possible if after this time $|i\rangle \leftrightarrow |j\rangle$, i.e. each site undergoes PST to its mirror-symmetric counterpart. To summarize: mirror-symmetry and a linear spectrum are together sufficient to ensure that the Hamiltonian supports PST.

Unfortunately, most Hamiltonians do not possess a perfectly linear spectrum, even if they are mirror symmetric. One may instead probe for IST, where the initial state at some site transfers to a different site with high probability. A naïve approach is to approximate all eigenvalues in the spectrum by rationals with the same common denominator, so that in principle the ratio condition (4) is automatically satisfied. Then in principle there should exist some time at which the Hamiltonian is almost site periodic, where initial states localized at a given site return with probability proportional to the accuracy of the rational approximation. By extension, if parity is a commuting operator then at half this time the probability at the mirror-symmetric vertex (the fidelity) should approach unity to within a similar error.

In fact the criteria for IST are slightly more involved than the naïve approach discussed above [23]. Recall that for a site-periodic Hamiltonian there exists a time $\lambda^{(n)}t/\hbar = 2\pi M_n$, $M_n \in \mathbb{Z}$ for all n so that the sum over n in Eq. (2) resolves to the identity. For almost site periodicity, and allowing for an arbitrary n -independent phase, this criterion would become $|\lambda^{(n)}t_P/\hbar + \varphi - 2\pi M_n| < \delta$, where $\delta \ll 1$. For reflection-symmetric Hamiltonians the



FIG. 1: Geometry of the model. Chain sites are labeled 1 through N , and the tunneling amplitude between adjacent sites is constant J (not labeled in the figure). The impurities consist of additional leaves at sites 3 and $N - 2$ labeled by $N + 1$ and $N + 2$, respectively. The amplitude to tunnel between chain and impurity sites is w .

eigenvalues of even and odd parity eigenstates interleave. At the IST time $t = t_P/2$, odd- n eigenstates map $|i\rangle$ to $|N - i + 1\rangle$ but with an additional π phase. The IST condition then reads

$$-\delta < \frac{\lambda^{(n)}t}{\hbar} - \alpha_n - 2\pi M_n < \delta, \quad n = 1, 2, \dots, N, \quad (5)$$

where $\alpha_n = \pi n - \varphi$. The first task would be to find integers M_n , the phase φ , and time t to satisfy this set of inequalities for each n at fixed δ . Once this is accomplished, one would calculate the output fidelity. Given initial occupation of vertex 1, the desired output vertex is N . The output fidelity is therefore

$$F(t) = |\langle N | e^{-iHt} | 1 \rangle|^2. \quad (6)$$

IST is said to occur at time t if $F(t)$ exceeds some minimum threshold, for example $F_{\min} = 0.9$.

III. MODEL AND BEHAVIOR

Consider an array of spin- $\frac{1}{2}$ particles, each confined to its own lattice site. As shown in Fig. 1, N sites are arranged in a one-dimensional chain with an additional spin connected to the third site from each end. Given a spin-spin coupling constant J along the chain (not explicitly labeled in the figure) and coupling constant w between the additional spins and their counterparts on the chain, the XY Hamiltonian reads

$$H = H_{1D} + H', \quad (7)$$

where

$$H_{1D} = \frac{J}{2} \sum_{i=1}^{N-1} (X_i X_{i+1} + Y_i Y_{i+1}) \quad (8)$$

corresponds to the one-dimensional uniform chain Hamiltonian and the Hamiltonian for the two additional impurity sites is

$$H' = \frac{w}{2} (X_3 X_{N+1} + Y_3 Y_{N+1} + X_{N-2} X_{N+2} + Y_{N-2} Y_{N+2}); \quad (9)$$

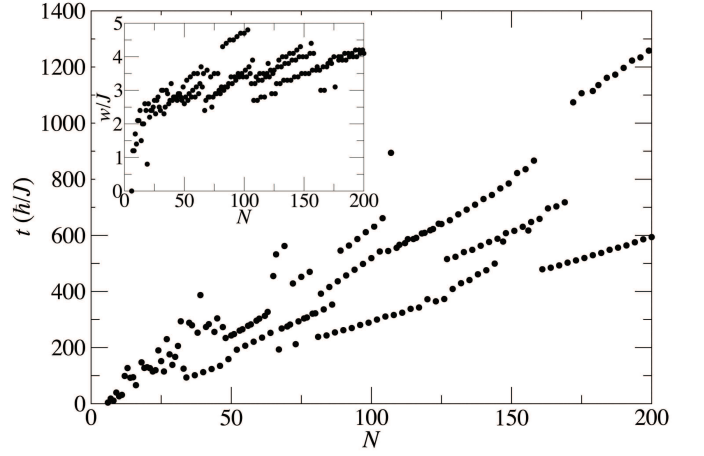


FIG. 2: The minimum time, in units of \hbar/J , for IST on the impurity-modified chain is shown as a function of the chain length for N between 6 and 200 sites. The inset shows the value of the impurity hopping parameter (impurity spin coupling constant) w associated with the minimum time, in units of the chain parameter J .

here $X = \sigma_x$ and $Y = \sigma_y$ are two-dimensional Pauli matrices. The total spin projection is a good quantum number and the Hamiltonian diagonalizes into blocks with a fixed number of excitations. Because only one excitation is required in order to effect state transfer, it is conventional to work in the single-excitation subspace [7, 35]. In this case, the spin Hamiltonian (7) is equivalent to a single particle hopping via a tight-binding Hamiltonian on an array with the same geometry, but with spin-coupling constants replaced by hopping amplitudes [39]:

$$H_{1D} = J \sum_{i=1}^{N-1} (|i\rangle\langle i+1| + |i+1\rangle\langle i|); \quad (10)$$

$$H' = w (|3\rangle\langle N+1| + |N-2\rangle\langle N+2| + \text{H.c.}). \quad (11)$$

Here, states $|i\rangle$ are unit vectors associated with site i , and H.c. stands for the Hermitian conjugate.

Determination of the conditions under which IST can occur (if any) for the geometry shown in Fig. 1 hinges on the diagonalization of the spin Hamiltonian (7) or alternatively (and more simply) the equivalent hopping Hamiltonian, Eqs. (10) and (11). To probe numerically for IST, we explicitly obtain the time-dependence of the probability on the output vertex using Eq. (2), and calculate the time-dependent fidelity $F(t)$, Eq. (6).

Figure 2 shows the minimum time for which IST is possible as a function of chain length N , for $6 \leq N \leq 200$. The results were obtained by looping over values of $\tilde{w} = w/J$ in the range $0 \leq \tilde{w} \leq 5$ in 0.1 increments for each value of N . For each \tilde{w} , the value of tJ/\hbar was increased in 0.1 increments until $F(t)$ was found to exceed $F_{\min} = 0.9$. Though IST is found to occur for many choices of t , only the lowest value of t for each \tilde{w} is shown

in Fig. 2; the value of \tilde{w} that minimizes t is shown in the inset. The data clearly show that the minimum time (and the impurity coupling constants associated with these) are nonmonotonic in N . There are intervals where the minimum time appears to scale linearly with N , but these are interrupted and interspersed with different trends. Likewise, the impurity coupling constants seem to scale roughly as \sqrt{N} , but the data are not clean.

In principle, one could try to determine the conditions on \tilde{w} that yield the absolute lowest-slope curve. This would yield a slightly modified spin chain where the IST time would scale linearly with length, albeit with restrictions on the values of N for which IST is possible. In this work, however, we pursue a different tack; namely, determining values of w valid for any instance of N and for which the IST time scales efficiently with N (i.e. as a power-law with N preferably with a low exponent). The analytical treatment discussed in the next section addresses this strategy.

IV. ANALYTICAL TREATMENT

While a complete analytical solution for arbitrary w (or for arbitrary w/J choosing J as the characteristic energy scale) appears difficult to obtain, approximate solutions may be obtained by solving the problem in the vicinity of the additional site(s) and matching to the bulk solution. First consider the left block in Fig. 1, consisting only of sites $i = \{1, 2, 3, 4, 5, N+1\}$ (the block with sites $i \rightarrow N-i+1$, $i = 1, 2, \dots, N$, and $N+1 \rightarrow N+2$ is wholly equivalent). Expressing the left block solution as

$$|\psi_L\rangle = \sum_{i=1}^4 a_i |i\rangle + a_{N+1} |N+1\rangle, \quad (12)$$

and operating with the left-block hopping Hamiltonian

$$H_L = J \sum_{i=1}^4 (|i\rangle\langle i+1| + |i+1\rangle\langle i|) + w(|3\rangle\langle N+1| + |N+1\rangle\langle 3|) \quad (13)$$

such that $H_L|\psi_L\rangle = \lambda|\psi_L\rangle$, one obtains

$$\{a_1, a_2, a_3, a_4, a_{N+1}\} = \frac{a_5}{\gamma} \left\{ 1, \tilde{\lambda}, \tilde{\lambda}^2 - 1, \frac{\tilde{\lambda}^2 - 1 + \gamma}{\tilde{\lambda}}, \tilde{w} \frac{\tilde{\lambda}^2 - 1}{\tilde{\lambda}} \right\}, \quad (14)$$

where $\gamma = 1 + \tilde{w}^2 - (3 + \tilde{w}^2)\tilde{\lambda}^2 + \tilde{\lambda}^4$, and $\tilde{w} = w/J$ and $\tilde{\lambda} = \lambda/J$ are the rescaled values of w and λ relative to the characteristic energy scale J .

The most important eigenvectors for IST are those with large amplitudes on the first and last sites of the chain, and by extension small amplitudes elsewhere. Small amplitude on the third site can be ensured if $\tilde{\lambda} \sim 1$. Likewise, for the amplitude on the fourth site to be small one requires $\gamma/\tilde{\lambda} \approx \gamma \ll 1$; this is possible if one chooses

$\tilde{w} \gg 1$. More concretely, suppose one sets $a_1 = \alpha a_4$ assuming $\alpha \gg 1$; using the explicit coefficients in Eq. (14) one obtains

$$\tilde{w} = \sqrt{\frac{\tilde{\lambda}_c(\alpha\tilde{\lambda}_c^3 - 2\alpha\tilde{\lambda}_c - 1)}{\alpha(\tilde{\lambda}_c^2 - 1)}}. \quad (15)$$

Setting $\tilde{\lambda}_c = 1 - \epsilon$ and expanding to lowest order in $\epsilon \sim 0$ gives

$$\tilde{w} \approx \pm \sqrt{\frac{1+\alpha}{2\alpha\epsilon}} \approx \pm \frac{1}{\sqrt{2\epsilon}}. \quad (16)$$

Note that necessarily $\epsilon > 0$ which ensures that $\tilde{\lambda}_c \lesssim 1$. Thus, the eigenvalue that ensures that the amplitude on the endpoint(s) is resonantly enhanced is

$$\tilde{\lambda}_c \approx 1 - \epsilon \approx 1 - \frac{1}{2\tilde{w}^2}. \quad (17)$$

The value of \tilde{w} can be positive or negative. Inserting this expression for $\tilde{\lambda}$ into Eq. (14) and again assuming $\tilde{w} \gg 1$ gives

$$\{a_1, a_2, a_3, a_4, a_{N+1}\} \propto \left\{ \tilde{w}^2, \tilde{w}^2, -1, -\frac{1}{4}, -\tilde{w} \right\}. \quad (18)$$

Note that the amplitudes on both the first and second sites of the chain are much larger than those elsewhere, which implies that any possible IST could equally originate at either of these sites. Thus, $\tilde{\lambda}_c$ is the eigenvalue for a state strongly localized in the vicinity of the impurity.

Next consider the solutions $|\psi_{1D}\rangle$ for the bulk one-dimensional chain H_{1D} , Eq. (10):

$$\langle i|\psi_{1D}^{(n)}\rangle = \sin(k_n i); \quad \tilde{\lambda}_{1D}^{(n)} = 2 \cos(k_n). \quad (19)$$

The reflection symmetry imposes the constraint that $\langle i|\psi_{1D}^{(n)}\rangle = \pm \langle N-i+1|\psi_{1D}^{(n)}\rangle$, i.e. that the solution is an eigenstate of the parity operator. Setting $\sin(k_n i) = -\sin(k_n i) \cos[k_n(N+1)] + \cos(k_n i) \sin[k_n(N+1)]$ for the even-parity case gives the conditions $\cos[k_n(N+1)] = -1$ and $\sin[k_n(N+1)] = 0$ which is satisfied by $k_n = \frac{\pi(2n+1)}{N+1}$, $n = 1, 2, \dots$. Likewise, the odd-parity solution requires $k_n = \frac{2\pi n}{N+1}$, so that overall $k_n = \frac{\pi n}{N+1}$, $n = 0, 1, \dots, N-1$. The invariance of the probability density under parity implies that all eigenvalues appear in plus/minus pairs, as $2 \cos(k_n) \rightarrow -2 \cos(k_n)$ for $n \rightarrow N+1-n$ ($k_n \rightarrow \pi - k_n$).

The bulk eigenvectors should automatically match the left-block solution (14) when $\tilde{w} = 0$. Whether using the bulk solution $\sin[\cos^{-1}(\tilde{\lambda}/2)i]$ from Eq. (19) or setting $\tilde{w} = 0$ in Eq. (14), one obtains the same result:

$$\{a_1, a_2, a_3, a_4\} \propto \left\{ 1, \tilde{\lambda}, \tilde{\lambda}^2 - 1, \tilde{\lambda}(\tilde{\lambda}^2 - 2) \right\}. \quad (20)$$

Alternatively, one can require that the bulk solution matches the amplitude on the last site of the left block:

$$\sin(4k_n) = \frac{\sin(5k_n)(\tilde{\lambda}^2 - 1 + \gamma)}{\gamma\tilde{\lambda}} = \frac{\sin(5k_n)\tilde{\lambda}(\tilde{\lambda}^2 - 2)}{\tilde{\lambda}^4 - 3\tilde{\lambda}^2 + 1}. \quad (21)$$

Using trigonometric identities it is straightforward to verify that this condition is (non-uniquely) satisfied by choosing $\tilde{\lambda} = \tilde{\lambda}^{(n)} = 2 \cos(k_n)$, as expected for the one-dimensional chain.

Return again to the $\tilde{w} \gg 1$ case, but now for generic $\tilde{\lambda}$ (keeping in mind that the $\tilde{\lambda} \sim 1$ are of particular interest, and that the reflection symmetry of the site array implies that all eigenvalues have negative counterparts $\tilde{\lambda} \rightarrow -\tilde{\lambda}$). The parameter γ in Eq. (14) becomes $\gamma \rightarrow \tilde{w}^2 (1 - \tilde{\lambda}^2)$. The left-block solution for $\tilde{w} \gg 1$ therefore becomes

$$\{a_1, a_2, a_3, a_4, a_{N+1}\} \rightarrow \left\{ 1, \tilde{\lambda}, \tilde{\lambda}^2 - 1, \frac{\tilde{w}^2(1 - \tilde{\lambda}^2) + \tilde{\lambda}^4 - 3\tilde{\lambda}^2 + 1}{\tilde{\lambda}}, \frac{\tilde{w}(\tilde{\lambda}^2 - 1)}{\tilde{\lambda}} \right\}, \quad (22)$$

neglecting unimportant prefactors. Comparison of Eqs. (20) and (22) reveals that the $\tilde{w} = 0$ and $\tilde{w} \gg 1$ wavefunctions match at all but the fourth site in the chain: if $\tilde{\lambda} \sim 1$ then $a_{N+1} \rightarrow 0$. This implies that the $\tilde{w} \gg 1$ eigenvalues almost coincide with those of the impurity-free chain. On the face of it, this is disappointing, as the bare chain cannot support efficient IST. Yet Eq. (17) clearly states that there always exists one eigenvalue for the localized state near the impurity that varies as $1 - 1/2\tilde{w}^2$, approaching unity asymptotically. The implication is that there must be (avoided) level crossings at finite \tilde{w} for every $\tilde{\lambda}^{(n)}$ that comes into resonance with the eigenvalue $\tilde{\lambda}_c$ of the localized state. It turns out that efficient IST hinges on the first of these avoided crossings.

Target eigenvalues are those in the vicinity of (but just below) unity, $\tilde{\lambda}^{(n)} = 2 \cos(k_n) - \epsilon \sim 1^-$, so that $k_n \gtrsim \pi/3$. That said, the $k_n = \pi n/(N+1)$ are discrete even in the limit of large N . There are therefore three different cases to consider: $N = 3m$ and $3m+1$ with $m = 2, 3, \dots$, and $3m-1$ with $m = 3, 4, \dots$. Consider first the $N = 3m$ case. The wave vectors of interest are indexed by $n = m + r$:

$$k_{m+r} = \frac{\pi(m+r)}{3m+1}, \quad (23)$$

where $r = 1, 2, \dots$ for $k_{m+r} > \pi/3$ to ensure that the associated eigenvalues $\tilde{\lambda}_r < 1$ (subscripts are now used to remind the reader that $r = 1$ corresponds to $n = 3m + r$). The $r = 1$ eigenvalue $\tilde{\lambda}_1 \approx 2 \cos(k_{m+1})$ must cross the critical eigenvalue $\tilde{\lambda}_c$ in Eq. (17) at some value of $\tilde{w} \gg 1$. The behavior of the system for large chains is of particular interest; expanding around $N = 3m \gg 1$ and large \tilde{w} , the levels cross when

$$1 - \frac{2\pi}{\sqrt{3}N} \approx 1 - \frac{1}{2\tilde{w}^2}, \quad (24)$$

which yields the critical impurity coupling constant

$$\tilde{w}_c \approx \pm \frac{3^{1/4}}{2\sqrt{\pi}} \sqrt{N} \approx \pm 0.37 \sqrt{N}. \quad (25)$$

Alternatively, consider the left-block eigenvector (14), which becomes

$$\{a_1, a_2, a_3, a_4, a_{N+1}\} \approx \left\{ \frac{\sqrt{3}}{2} + \frac{8\pi\tilde{w}^2}{N} + \mathcal{O}\left(\frac{\tilde{w}^4}{N^2}\right), \frac{\sqrt{3}}{2} + \frac{8\pi\tilde{w}^2}{N} + \mathcal{O}\left(\frac{\tilde{w}^4}{N^2}\right), -\frac{8\pi}{N} + \mathcal{O}\left(\frac{\tilde{w}^2}{N^2}\right), -\frac{\sqrt{3}}{2} - \frac{16\pi}{3N} + \mathcal{O}\left(\frac{\tilde{w}^2}{N^2}\right), -\frac{8\pi\tilde{w}}{N} + \mathcal{O}\left(\frac{\tilde{w}^3}{N^2}\right) \right\}. \quad (26)$$

Clearly, the expansions above are analytic only if \tilde{w} varies with N more slowly than \sqrt{N} (or one could obtain a convergent series by expanding the solution (14) in N/\tilde{w} for \tilde{w} a polynomial in N with exponent greater than $1/2$). The critical case $\tilde{w}_c = \alpha\sqrt{N}$ is therefore of particular interest. For large N one obtains

$$\{a_1, a_2, a_3, a_4, a_{N+1}\} \approx \left\{ \frac{\sqrt{3}}{2\left(1 - \frac{4\pi\alpha^2}{\sqrt{3}}\right)}, \frac{\sqrt{3}}{2\left(1 - \frac{4\pi\alpha^2}{\sqrt{3}}\right)}, -\frac{2\pi}{N\left(1 - \frac{4\pi\alpha^2}{\sqrt{3}}\right)}, -\frac{\sqrt{3}}{2}, -\frac{2\pi\alpha}{\sqrt{N}\left(1 - \frac{4\pi\alpha^2}{\sqrt{3}}\right)} \right\}, \quad (27)$$

which matches the bulk solution at the fourth site. The amplitudes on the first and second sites are strongly enhanced relative to the others if one sets $1 - \frac{4\pi\alpha^2}{\sqrt{3}} = 0$ or $\alpha = 3^{1/4}/2\sqrt{\pi}$, consistent with Eq. (25). Equivalently, the state (27) has maximal overlap with the state (18) when the first two amplitudes above equal $\tilde{w}^2 = \alpha^2 N$, which also occurs for $\alpha = 3^{1/4}/2\sqrt{\pi}$.

The $N = 3m + 1$ and $N = 3m - 1$ cases proceed analogously. For $N = 3m + 1$ for large N one obtains the critical impurity coupling constant

$$\tilde{w}_c \approx \pm \frac{3^{1/4}}{\sqrt{2\pi}} \sqrt{N} \approx 0.53 \sqrt{N}, \quad (28)$$

while for $N = 3m - 1$ in the same limit one obtains

$$\tilde{w}_c \approx \frac{1}{3^{1/4}\sqrt{2\pi}} \sqrt{N} \approx 0.30 \sqrt{N}. \quad (29)$$

While all critical impurity coupling constants scale as \sqrt{N} , the prefactor depends on the particular choice of $N \pmod{3}$, $N + 1 \pmod{3}$, or $N - 1 \pmod{3}$.

Return again to the $N = 3m$ case. As \tilde{w} is increased through the critical value (25), the $2 \cos(k_{m+1})$ eigenvalue must exhibit an avoided crossing with $\tilde{\lambda}_c$, while its associated eigenvector strongly mixes with the next odd-parity state with eigenvalue λ_3 . Likewise, the eigenvalue $\tilde{\lambda}_2$ of the first relevant even-parity state should also follow Eq. (17) for large \tilde{w} , while strongly mixing with the $\tilde{\lambda}_4$ state for intermediate \tilde{w} at the second avoided crossing in the vicinity of $2 \cos(k_{m+3})$, etc. That said, presumably the $\tilde{\lambda}_2$ state only mixes weakly with the $\tilde{\lambda}_4$ state near the first avoided crossing (and of course not

at all with the $\tilde{\lambda}_1$ and $\tilde{\lambda}_3$ states due to parity), which should occur for much larger values of \tilde{w} than the second avoided crossing. With this assumption, $\tilde{\lambda}_2$ follows Eq. (17) throughout the first level crossing.

By inference, therefore, only three states are relevant to the first avoided crossing, corresponding to eigenvalues indexed by $r = 1, 2, 3$. The same phenomenon also applies to the $N = 3m + 1$ and $N = 3m - 1$ cases, but the avoided crossing occurs for different k labels and therefore at different energies. Importantly, all three states involved in the avoided crossing at \tilde{w}_c have strongly enhanced amplitude on the first and last site of the chain (as well as the second and second-from last), of order unity after normalization. All other states will be far off-resonant, and will have low amplitudes on the endpoints proportional to the overall normalization constant for bulk eigenvectors $\propto \sqrt{2/N}$. But the sum of outer products of eigenvectors must resolve to the identity. This implies that as $N \rightarrow \infty$, no off-resonant eigenvectors will contribute to the state transfer: the sum in Eq. (2) will only include resonant eigenvectors. Because only three equally-spaced eigenvalues are involved (plus their negatives), the state transfer must be asymptotically perfect.

Obtaining an analytical estimate of the energy splitting at the critical impurity coupling constant is not as straightforward as it appears. The usual method would be to start with eigenfunctions $|\psi_{1D}^{(m+1)}\rangle$ and $|\psi_{1D}^{(m+3)}\rangle$ of the unperturbed Hamiltonian (10) and then calculate the mixing caused by the perturbation (11), i.e. the off-diagonal term of the mixing matrix $\Delta \equiv \langle \psi_{1D}^{(m+1)} | H' | \psi_{1D}^{(m+3)} \rangle$. The impurities have no support on the bare chain, however, so in principle the energy splitting $\Delta = 0$. One can nevertheless estimate Δ as follows. The contribution to Δ from all the chain sites will be zero, as the unperturbed eigenfunctions are orthogonal. At \tilde{w}_c , the amplitude on the impurity site for the $k = m + 1$ state is $-1/2\tilde{w}_c = -\sqrt{\pi}/3^{1/4}\sqrt{N}$ after normalization (which is dominated by the amplitudes on the first two and last two sites of the chain). Likewise, the amplitude on the impurity site for the $k = m + 3$ state is $-\sqrt{2/N}(4\sqrt{\pi}/3^{3/4}\sqrt{N}) = -4\sqrt{2\pi}/3^{3/4}N$ including the normalization factor for $\sin(k_n)$ eigenfunctions. Because the action of the Hamiltonian on this site returns the same amplitude (the energy is almost unity), one obtains

$$\Delta \approx \frac{4\sqrt{2\pi}}{3^{3/4}N} \frac{\sqrt{\pi}}{3^{1/4}\sqrt{N}} = \frac{4\sqrt{2\pi}}{3N^{3/2}}. \quad (30)$$

While the coefficient is probably not that accurate, the analytics suggest that the energy splitting at the avoided crossing scales with the chain length as $N^{-3/2}$. The IST time should therefore scale as $t_{\text{IST}} \sim N^{3/2}$.

At this juncture the reader might well be wondering what is special about adding impurities to the third and third-from-last sites of the chain. Suppose that the impurities were instead located on the second and second-from-last sites of the chain. The left-block state, analo-

gous to Eq. (14) is found to be

$$\{a_1, a_2, a_3, a_{N+1}\} = \frac{a_4}{\gamma\tilde{\lambda}} \left\{ 1, \tilde{\lambda}, \tilde{\lambda}^2 - 1 - \tilde{w}^2, \tilde{w} \right\}, \quad (31)$$

where $\gamma = 2 - \tilde{\lambda}^2 - \tilde{w}^2$. The amplitude on the first site can be made larger than in the bulk only if $\tilde{\lambda} \sim 1$ and $\tilde{w} \sim 0$. The second condition is unfortunately equivalent to the unmodified chain, and is therefore not useful. Consider instead impurities on the fourth and fourth-from-last sites of the chain. The left-block solution is now

$$\begin{aligned} &\{a_1, a_2, a_3, a_4, a_5, a_{N+1}\} \\ &= \frac{a_6\tilde{\lambda}}{\gamma} \left\{ 1, \tilde{\lambda}, \tilde{\lambda}^2 - 1, \tilde{\lambda}(\tilde{\lambda}^2 - 2), \tilde{\lambda}^2 - 2 + \gamma, \tilde{w}(\tilde{\lambda}^2 - 2) \right\}, \end{aligned} \quad (32)$$

where $\gamma = 3 + 2w^2 - (4 + w^2)\tilde{\lambda}^2 + \tilde{\lambda}^4$. Following the analysis above, small amplitude on the fourth and fifth sites requires $\tilde{w} \gg 1$ and $\tilde{\lambda} \approx \sqrt{2} - 1/2\sqrt{2}w^2$. To leading order in \tilde{w} one obtains

$$\begin{aligned} &\{a_1, a_2, a_3, a_4, a_5, a_{N+1}\} \\ &\approx \left\{ \tilde{w}^2, \sqrt{2}\tilde{w}^2, \tilde{w}^2, -\sqrt{2}, -\frac{9}{8}, -\tilde{w} \right\}. \end{aligned} \quad (33)$$

Just as for impurities on sites $i = 3$ and $N - i + 2$, there is a strong enhancement of amplitude on the first and last sites. This enhancement is now shared with four other sites ($i = 2, 3, N - 1$, and $N - 2$), however, decreasing the total amplitude available on the target sites. This trend continues as the impurities move further from the ends of the chain. Thus, adding impurities to the third and third-from-last sites is optimal.

V. NUMERICAL RESULTS

The strategy pursued in this work is to determine if there exist values of $\tilde{w}(N)$ that allow APST to occur for all N , but perhaps not at the absolute minimum time allowable. Using the analytical results of the previous section as a guide, for particular values of \tilde{w} one expects that for eigenvalues $\tilde{\lambda}^{(n)} \lesssim 1$ of the Hamiltonian the associated eigenvectors $|\psi^{(n)}\rangle$ will have a large overlap with the first and last sites of the chain. If the eigenvalues are reverse ordered so that $\tilde{\lambda}^{(n)} \geq \tilde{\lambda}^{(n+1)}$ for $n = 1, 2, \dots, N - 1$, then there exist values of $n \gtrsim N/3$ where $\tilde{\lambda}^{(n)} \lesssim 1$. Define $N \equiv 3m + p$, where $p \in \{-1, 0, 1\}$. Then one can define $\tilde{\lambda}_q = \tilde{\lambda}^{(q+m)}$ which are all less than unity for $q = 1, 2, \dots$, and their associated eigenvectors $|\psi_q\rangle$. Then IST should result for values of \tilde{w} where the eigenvalues and eigenvectors satisfy the following two criteria:

$$\left| \frac{\Delta_2 - \Delta_1}{\Delta_1} \right| \leq \epsilon; \quad (34)$$

$$2 \sum_{q=1}^3 |\langle \psi_q | 1 \rangle|^2 \geq f, \quad (35)$$

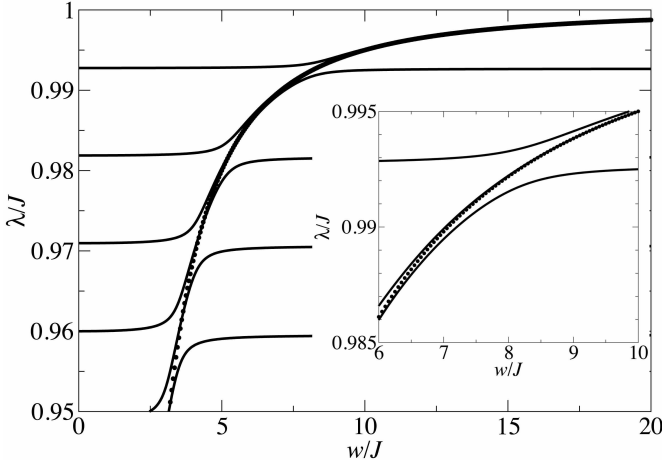


FIG. 3: The first few eigenvalues $\tilde{\lambda}_q = \lambda^{q+m}/J$ smaller than unity ($q = 1, 2, \dots, 6$) are shown as a function of the impurity coupling parameter $\tilde{w} = w/J$ for chain length $N = 3m = 501$ (black lines). Also shown is the left-block eigenvalue $\tilde{\lambda} = \lambda/J = 1 - 1/2\tilde{w}^2$ (dotted curve). The first avoided level crossing, closest to unity, is magnified in the inset.

where the two successive eigenvalue gaps are $\tilde{\Delta}_1 = \tilde{\lambda}_1 - \tilde{\lambda}_2$ and $\tilde{\Delta}_2 = \tilde{\lambda}_2 - \tilde{\lambda}_3$, and $\epsilon \ll 1$ and $f \lesssim 1$ are free parameters.

The Hamiltonian H was diagonalized for each chain length N in the range $6 \leq N \leq 501$. Figure 3 shows the representative behavior of the first few eigenvalues less than unity as a function of the impurity coupling $\tilde{w} = w/J$ for $N = 3m = 501$. The salient features predicted by the analytical treatment are readily observed here. The bare-chain eigenvalues $\tilde{\lambda}_q^0 = 2 \cos[\pi(q+m)/(N+1)]$ (for $\tilde{w} = 0$) are crossed by the eigenvalue $\tilde{\lambda}_c = 1 - 1/2\tilde{w}^2$ of the localized state at finite w , (almost) recovering their values for large \tilde{w} . The $q = 1$ and $q = 2$ eigenvalues both follow $\tilde{\lambda}_c$ for large \tilde{w} , while the $q = 3$ eigenvalue approaches $2 \cos[\pi(1+m)/(N+1)]$ in the same limit.

The strong mixing between the localized and extended bulk eigenvectors gives rise to avoided crossings, and the first such crossing (closest to unity) is shown in the inset of Fig. 3. As expected, the $q = 2$ eigenvalue closely follows $\tilde{\lambda}_c$ through the first avoided crossing, as it only weakly mixes with the $q = 4$ eigenvalue here. At the value of \tilde{w} where $\tilde{\lambda}_c \approx \tilde{\lambda}_2 = \tilde{\lambda}_1^0$, the $\tilde{\lambda}_1$ and $\tilde{\lambda}_3$ eigenvalues are split equally above and below $\tilde{\lambda}_2$. Thus, \tilde{w}_c both defines the point at which $\tilde{\lambda}_c = \tilde{\lambda}_1$ and the point at which the energy gaps coincide, $\tilde{\Delta}_1 = \tilde{\Delta}_2 \equiv \tilde{\Delta}$.

Figure 3 also suggests that there are multiple values of the impurity hopping parameter that give rise to eigenvalue resonances. The second avoided crossing occurs when $\tilde{\lambda}_c = \tilde{\lambda}_2$. For the $N = 501$ case displayed here, the analog of result (25) for the second avoided crossing is $\tilde{w}'_c = (3^{1/4}/\sqrt{10\pi})\sqrt{N} \approx 0.23\sqrt{N}$. While the qualitative behavior of the eigenvalue splitting is similar, one would expect a lower IST output fidelity as the maximum amplitude on the endpoint sites is now approximately

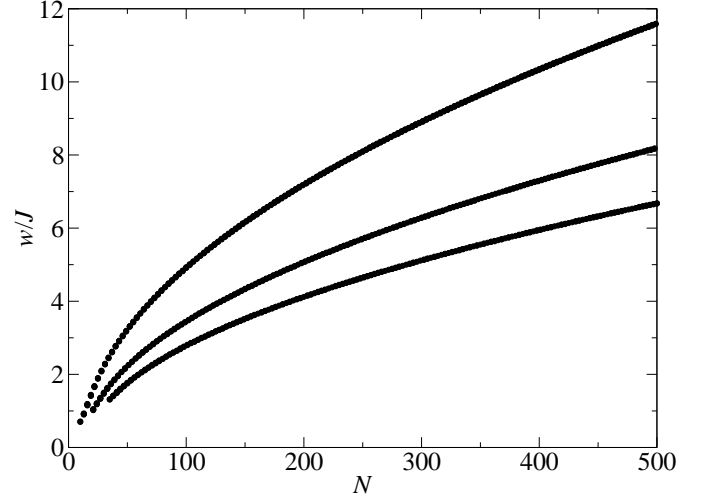


FIG. 4: The numerical value of the impurity coupling constant $\tilde{w} = w/J$ ensuring that the eigenvalues at the first level crossing are equally spaced are shown as a function of the chain length N . Top, middle, and lower curves correspond to $N = 3m + 1$, $3m$, and $3m - 1$ (m integer), respectively. All curves closely follow $\tilde{w} \sim \sqrt{N}$ for large N .

63% lower than for the first avoided crossing according to Eq. (18).

Eq. (34) specifies that the spacing between successive eigenvalues just less than unity be equal to within some tolerance ϵ . Figure 4 shows the value of impurity parameter $\tilde{w} = w/J$ satisfying Eq. (34) at the first avoided crossing to a tolerance $\epsilon = 10^{-10}$, for $6 \leq N \leq 501$. There are three distinct curves, depending on the value of N . The lowest, middle, and upper curves correspond to $N + 1 \pmod{3}$, $N \pmod{3}$, and $N - 1 \pmod{3}$, respectively. For the largest chain sizes considered, in the range $400 \leq N \leq 500$, each of these curves is well fit (correlation coefficient > 0.999) by a power law that closely resembles the analytical results, Eqs. (28), (25), and (29), respectively: $\tilde{w} \approx 0.48N^{0.51}$ for $N = 3m + 1$, $\tilde{w} \approx 0.33N^{0.52}$ for $N = 3m$, and $\tilde{w} \approx 0.27N^{0.52}$ for $N = 3m - 1$. In all cases, the results are compatible with a \sqrt{N} scaling for large N . That said, the prefactors obtained numerically are all found to be below the analytical predictions by approximately 10%; it is possible that the correspondence between analytics and numerics would tighten up for larger N .

Under the assumption that only the first three eigenvectors $|\psi_q\rangle$ with eigenvalues λ_q just below unity (and their negative counterparts) contribute to the transfer dynamics, the IST time can be predicted using Eq. (3). Following the discussion in Sec. II, imperfect site periodicity occurs at a time $t = 2\pi\hbar/(\lambda_1 - \lambda_2) = 2\pi\hbar/\Delta_1$, and parity conservation implies that the imperfect state transfer time is half this, $t_{\text{IST}} \equiv \pi\hbar/\Delta_1 = (\pi\hbar/J)/\tilde{\Delta}_1$. In rescaled time units $t = (\hbar/J)\tilde{t}$, one obtains $\tilde{t}_{\text{IST}} \equiv \pi/\tilde{\Delta}$, where $\tilde{\Delta} = \tilde{\Delta}_1 = \tilde{\Delta}_2$. The state transfer times t_{IST} are shown as a function of the chain length in the range

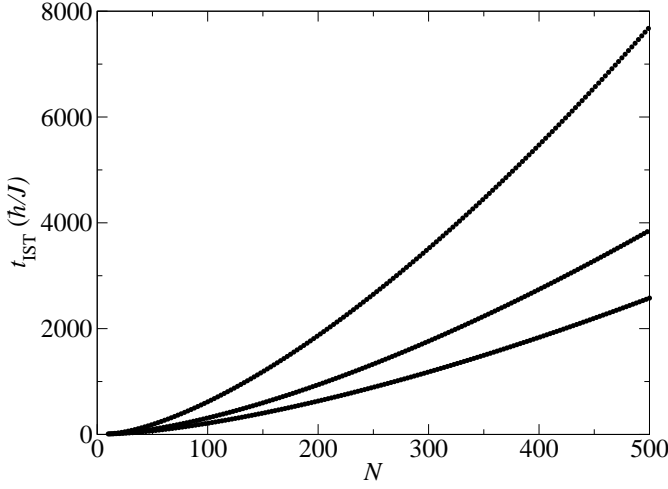


FIG. 5: The numerical estimate of the imperfect state transfer time t_{IST} , based on the value of the resonant energy gaps, is shown as a function of the chain length N . Top, middle, and lower curves correspond to $N = 3m + 1$, $3m$, and $3m - 1$ (m integer), respectively. All curves closely follow $t_{\text{IST}} \sim N^{3/2}$ for large N .

$10 \leq N \leq 501$ in Fig. 5. These times are based on the energy gaps $\tilde{\Delta}_1 = \tilde{\Delta}_2$ at the critical weight plotted in Fig. 4. As was the case for the critical weights, the IST time scales differently depending on the value of $N \pmod{3}$. For $N = 3m$, the numerical results are best fit by the function $\tilde{t}_{\text{IST}} \approx 0.29N^{1.53}$ for large integer m ; for $N = 3m + 1$ and $3m - 1$ one obtains $\tilde{t}_{\text{IST}} \approx 0.57N^{1.53}$ and $\tilde{t}_{\text{IST}} \approx 0.20N^{1.52}$, respectively. The power laws are all consistent with a $N^{3/2}$ scaling of time, as predicted by the analytics discussed in the previous section. The prefactors also appear to scale roughly with those for the critical weights.

It is worthwhile to investigate the IST dynamics governed by Eq. (2) more closely. Keeping in mind that $|\psi_1\rangle$ and $|\psi_3\rangle$ have even parity while $|\psi_2\rangle$ has odd parity (and vice versa for $\lambda_q \rightarrow -\lambda_q$), so that for example $\langle\psi_1|1\rangle = \langle\psi_1|N\rangle$ while $\langle\psi_2|1\rangle = -\langle\psi_2|N\rangle$, one obtains

$$\begin{aligned} \langle N|e^{-iHt/\hbar}|1\rangle &\approx -2i \sin[(\lambda_2 + \Delta)t/\hbar] |\langle\psi_1|1\rangle|^2 \\ &\quad + 2i \sin[\lambda_2 t/\hbar] |\langle\psi_2|1\rangle|^2 \\ &\quad - 2i \sin[(\lambda_2 - \Delta)t/\hbar] |\langle\psi_3|1\rangle|^2, \end{aligned} \quad (36)$$

keeping only resonant eigenvectors in the sum. Choosing t such that the coefficients of each $|\langle\psi_q|1\rangle|^2$ term are equal, one obtains $t_{\text{IST}} = \pi\hbar/\Delta$, as expected. Then Eq. (36) becomes

$$\begin{aligned} \langle N|e^{-iHt/\hbar}|1\rangle &= 2i \sin\left(\frac{\pi\lambda_2}{\Delta}\right) \sum_{q=1}^3 |\langle\psi_q|1\rangle|^2 \\ &\approx i \sin\left(\frac{\pi\lambda_2}{\Delta}\right), \end{aligned} \quad (37)$$

where the second line is obtained by assuming that only these eigenvectors (and their negative-eigenvalue

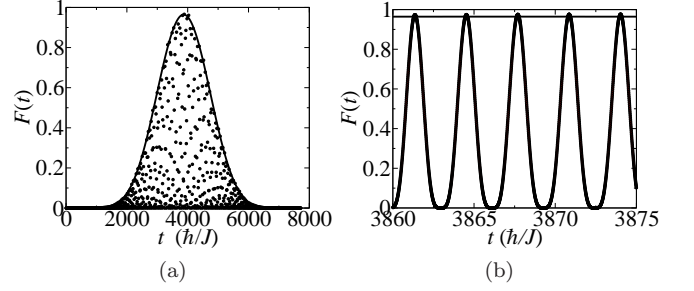


FIG. 6: The IST fidelity $F(t)$ is plotted as a function of time for $N = 501$ at the critical impurity coupling constant $\tilde{w} \approx 8.2$. Dots correspond to numerical data while the solid lines correspond to the envelope of the output fidelity including only contributions from the critical eigenvectors. The slow increase in fidelity through the IST time $t_{\text{IST}} = \pi/\tilde{\Delta} \approx 3867$ is shown in (a). A close-up of the behavior in the vicinity of t_{IST} is shown in (b). Note that the dots are so closely spaced here that they resemble an oscillating line, whereas the solid line appears almost horizontal.

counterparts) resolve the identity. Equation (37) appears to suggest that the maximum fidelity is $F(t_{\text{IST}}) = \sin^2(\pi\lambda_2/\Delta) \approx \sin^2(\pi/\tilde{\Delta})$. The interference arises from the fact that while the first three eigenvalues below unity become approximately evenly spaced by Δ at resonance, the corresponding second set of approximately evenly spaced eigenvalues above -1 are not necessary an integer number of Δ away from the first set.

High-fidelity IST is in fact possible if the time is chosen to be slightly above or below π/Δ . For times in the vicinity of $t \sim t_{\text{IST}}$, Eq. (3) becomes approximately

$$\begin{aligned} \langle N|e^{-iHt/\hbar}|1\rangle &\approx \sum_{q=1}^3 \left(-e^{-i\lambda_2 t/\hbar} |\langle\psi_q|1\rangle|^2 \right. \\ &\quad \left. + e^{i\lambda_2 t/\hbar} |\langle\psi'_q|1\rangle|^2 \right). \end{aligned} \quad (38)$$

Here, $|\psi'_q\rangle$ are the eigenvectors corresponding to the first eigenvalues above -1 (i.e. for $\lambda_q \rightarrow -\lambda_q$); note that $\langle 1|\psi'_q\rangle = \langle 1|\psi_q\rangle$ while $\langle N|\psi'_q\rangle = -\langle N|\psi_q\rangle$. The right-hand side of Eq. (38) is proportional to unity if time is chosen to be $t = (2n - 1)\pi\hbar/2\lambda_2$, or $\tilde{t} = -\pi/2 + r\pi$ where r is an arbitrary integer. For times near t_{IST} , the probability on the output site varies from zero to near unity with a period $\pi \ll t_{\text{IST}}$. One can therefore choose a time in the vicinity of t_{IST} at which the fidelity should approach unity.

Figure 6 shows the IST fidelity $F(t)$, defined in Eq. (6), as a function of time for the particular case of $N = 501$ using the optimal impurity coupling constant $\tilde{w}_c \approx 8.197$. As expected, $F(t)$ reaches a maximum value at a time near $\tilde{t}_{\text{IST}} \approx 3867.44$, though the function oscillates rapidly throughout this slow variation. The behaviour of the fidelity including only resonant eigenvectors in the sum (2) is shown for comparison; only the envelope of the fidelity is plotted for clarity, as this exhibits the same

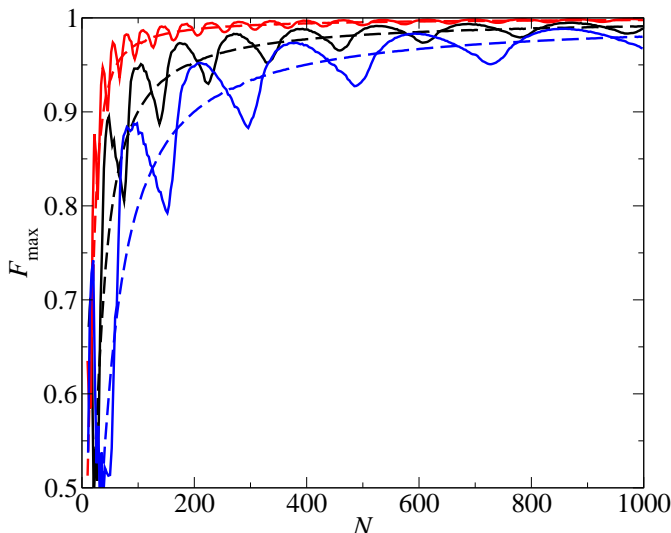


FIG. 7: (color online) The maximum fidelity F_{\max} for the state transfer between endpoints is shown as a function of the chain length N . Red, black, and blue curves correspond to $N = 3m + 1$, $3m$, and $3m - 1$, $3 \leq m \leq 333$, respectively. Solid lines depict the exact fidelity while dashed lines represent the result including only the six resonant eigenvectors.

fast oscillation of the full data. Figure 6(a) clearly shows that the time evolution of the output fidelity is governed almost completely by the resonant eigenvectors. A close-up of the time sequence in the vicinity of $t \sim t_{\text{IST}}$ reveals the fast oscillation of $F(t)$; the period is found to be $\tilde{T}_{\text{fast}} \approx 3.16$ which is close to the predicted value of π . While $F(t_{\text{IST}}) \approx 0.858$, the output fidelity actually attains a maximum $F_{\max} \approx 0.975$ at the slightly longer time $\tilde{t} = 3867.70$. This maximum is attained for many \tilde{T}_{fast} periods in the vicinity of \tilde{t}_{IST} . In fact, the maximum fidelity for the full dynamics slightly exceeds the value $F \approx 0.964$ obtained from including only the resonant eigenvectors.

The maximum fidelity F_{\max} for quantum state transfer is shown as a function of N in Fig. 7 for $10 \leq N \leq 1000$. The data are obtained by scanning the fidelity in the temporal region $\tilde{t}_{\text{IST}} - 3\tilde{T}_{\text{fast}} \leq \tilde{t} \leq \tilde{t}_{\text{IST}} + 3\tilde{T}_{\text{fast}}$ and recording the maximum result for each N . The exact results F_{\max} , where all eigenvectors are included in the sum (2), are shown as solid lines; the fidelities F'_{\max} when the sum is restricted only to resonant eigenvectors is shown as dashed lines. While N -dependent oscillations are evident in the exact results, the amplitudes decrease and the wavelengths increase with N ; more important, though, their centers consistently follow the restricted fidelity curves. The restricted fidelities therefore provide an accurate representation of the exact fidelities in the thermodynamic limit $N \rightarrow \infty$. The values of restricted fidelities for large N in the range $800 \leq N \leq 1000$ are

found to follow

$$F'_{\max} \approx \begin{cases} 1 - \frac{2.34}{N^{1.01}} & N = 3m + 1; \\ 1 - \frac{11.4}{N^{1.04}} & N = 3m; \\ 1 - \frac{17.3}{N^{0.98}} & N = 3m - 1, \end{cases} \quad (39)$$

with suitably chosen integer m . Thus, the IST fidelity approaches unity in the thermodynamic limit, i.e. the quantum state transfer is asymptotically perfect. According to the numerics, the state transfer error scales as $1 - F \propto N^{-1}$ for large N .

VI. DISCUSSION AND CONCLUSIONS

In this work we have shown that asymptotically perfect quantum state transfer is possible in uniform chains that have been modified by the addition of two impurities, coupled to the uniform chain at the third and third-from-last sites with strength w . Choosing $w \propto \sqrt{N}$, the state localized in the vicinity of the impurity can be tuned into resonance with chain extended states. The associated avoided level crossing gives rise to eigenstates with large overlaps with the chain endpoints and with eigenvalues whose spacings become approximately equal. The approximate linear spectrum together with reflection symmetry yields approximately perfect state transfer, in a time that scales efficiently with length, as $t_{\text{IST}} \propto N^{3/2}$. Indeed, the fidelity is found to approach unity in the thermodynamic limit $N \rightarrow \infty$, with error scaling as $1 - F \propto N^{-1}$. To our knowledge, this is the only configuration with no external time-dependent or local control, where a uniform chain can be made to transfer quantum information perfectly in the limit of large system size,

While the central insights obtained from the analytical investigations are validated by the explicit calculations, the numerical results reveal additional information and display some important features. First and foremost, the detailed dependence of the energy splitting on N at resonance (equivalently the amplitude of the $t_{\text{IST}} \propto N^{3/2}$ scaling) was only readily available numerically. Second, the exact time-dependence of the output probability was found to oscillate rapidly (with period $\pi\hbar/J$) in addition to the slow evolution toward maximum fidelity in the vicinity of t_{IST} , independent of N . This means that in a practical experiment (with N large but fixed) the timing would have to be tested over a range of times $|t - t_{\text{IST}}| \leq (\pi/2)(\hbar/J)$ prior to using this device to transfer unknown quantum information. Third, the exact value of the maximum fidelity is found to follow the value obtained by including only the critical eigenvectors, but for smaller N it displays pronounced oscillations. The amplitude and frequency of these oscillations decreases steadily with N , so that in the thermodynamic limit the maximum fidelity is completely dominated by the resonant eigenvectors.

Given that the high-fidelity transfer is a direct consequence of a resonance between the localized and extended states, one might expect the model to be robust

against random small errors in the chain coupling constants around J . The errors would shift the frequencies of the extended states, so that a new value of w would need to be found to bring them back into resonance. While this is possible in principle, in practice finding the best value of w and time could be difficult; if the errors are time-dependent the situation is even worse. Unfortunately, numerical calculations suggest that the value of F falls precipitously with noise if w and t are both fixed at their optimal noise-free value. Given $J_{i,i+1} = J \pm \delta J_{i,i+1}$ with random values $|\delta J_{i,i+1}| \leq x$, we find for $N = 501$ that the average fidelity drops to $\overline{F} \sim 0.1$ for $x \approx 0.01$.

Previous studies of perfect quantum state transfer have shown that if the evolution of a particle on a graph exhibits PST then so will its evolution on Cartesian powers of this graph [19]. Because the Cartesian square and cube of the uniform chain are two and three-dimensional lattices, respectively, one could in principle extend the

current model to exhibiting PST from corner to corner of regular lattices in any dimension. That said, the two impurities in one dimension translate to an unwieldy $4N$ impurities in two dimensions. Rather, one could envisage arranging a sequence of impurities forming a half box of length three centered at each corner. This would ensure the presence of a localized state near the endpoints, which could again be tuned into resonance through a suitable adjustment of the impurity coupling parameters. We hope to explore this idea further in future work.

Acknowledgments

This work was supported by the Natural Sciences and Engineering Research Council of Canada.

-
- [1] N. Gisin and R. Thew, *Nature Photonics* **1**, 165 (2007).
 - [2] M. A. Nielsen and I. L. Chuang, *Quantum Computation and Quantum Information: 10th Anniversary Edition* (Cambridge University Press, New York, NY, USA, 2011), 10th ed.
 - [3] D. D. Awschalom, L. C. Bassett, A. S. Dzurak, E. L. Hu, and J. R. Petta, **339**, 1174 (2013).
 - [4] M. W. Doherty, N. B. Manson, P. Delaney, F. Jelezko, J. Wrachtrup, and L. C. Hollenberg, *Physics Reports* **528**, 1 (2013).
 - [5] A. Kay, *Int. J. Quantum Inform.* **8**, 641 (2010).
 - [6] M. Christandl, N. Datta, A. Ekert, and A. J. Landahl, *Phys. Rev. Lett.* **92**, 187902 (2004).
 - [7] M. Christandl, N. Datta, T. C. Dorlas, A. Ekert, A. Kay, and A. J. Landahl, *Phys. Rev. A* **71**, 032312 (2005).
 - [8] Y. Wang, F. Shuang, and H. Rabitz, *Phys. Rev. A* **84**, 012307 (2011).
 - [9] L. Vinet and A. Zhedanov, *Phys. Rev. A* **85**, 012323 (2012).
 - [10] I. S. N. Saxena, S. Severini, *Int. J. Quantum Inform.* **5**, 417 (2007).
 - [11] C. Facer, J. Twamley, and J. Cresser, *Phys. Rev. A* **77**, 012334 (2008).
 - [12] A. Bernasconi, C. Godsil, and S. Severini, *Phys. Rev. A* **78**, 052320 (2008).
 - [13] M. A. Jafarizadeh and R. Sufiani, *Phys. Rev. A* **77**, 022315 (2008).
 - [14] R. J. Angeles-Canul, R. M. Norton, M. C. Opperman, C. C. Paribello, M. C. Russell, and C. Tamon, *Int. J. Quantum Comput.* **7**, 1429 (2009).
 - [15] M. Bašić, M. D. Petković, and D. Stevanović, *Appl. Math. Lett.* **22**, 1117 (2009).
 - [16] M. Bašić and M. D. Petković, *Appl. Math. Lett.* **22**, 1609 (2009).
 - [17] R. J. Angeles-Canul, R. M. Norton, M. C. Opperman, C. C. Paribello, M. C. Russell, and C. Tamon, *Quantum Inf. Comput.* **10**, 325 (2010).
 - [18] Y. Ge, B. Greenberg, O. Perez, and C. Tamon, *Int. J. Quantum Inform.* **9**, 823 (2011).
 - [19] R. Bachman, E. Fredette, J. Fuller, M. Landry, M. Opperman, C. Tamon, and A. Tollefson, *Quantum Inf. Comput.* **12**, 293 (2012).
 - [20] J. Brown, C. Godsil, D. Mallory, A. Raz, and C. Tamon, *Quant. Inf. Comput.* **13**, 511 (2013).
 - [21] C. Godsil, *Discrete Math.* **6**, 129 (2012).
 - [22] C. Godsil, S. Kirkland, S. Severini, and J. Smith, *Phys. Rev. Lett.* **109**, 050502 (2012).
 - [23] L. Vinet and A. Zhedanov, *Phys. Rev. A* **86**, 052319 (2012).
 - [24] R. Sousa and Y. Omar, *New Journal of Physics* **16**, 123003 (2014).
 - [25] A. Wójcik, T. Łuczak, P. Kurzyński, A. Grudka, T. Gdala, and M. Bednarska, *Phys. Rev. A* **72**, 034303 (2005).
 - [26] L. Campos Venuti, S. M. Giampaolo, F. Illuminati, and P. Zanardi, *Phys. Rev. A* **76**, 052328 (2007).
 - [27] E. B. Fel'dman, E. I. Kuznetsova, and A. I. Zenchuk, *Phys. Rev. A* **82**, 022332 (2010).
 - [28] L. Bianchi, T. J. G. Apollaro, A. Cuccoli, R. Vaia, and P. Verrucchi, *New Journal of Physics* **13**, 123006 (2011).
 - [29] N. Y. Yao, L. Jiang, A. V. Gorshkov, Z.-X. Gong, A. Zhai, L.-M. Duan, and M. D. Lukin, *Phys. Rev. Lett.* **106**, 040505 (2011).
 - [30] T. J. G. Apollaro, L. Bianchi, A. Cuccoli, R. Vaia, and P. Verrucchi, *Phys. Rev. A* **85**, 052319 (2012).
 - [31] A. Zwick, G. A. Álvarez, J. Stolze, and O. Osenda, *Phys. Rev. A* **85**, 012318 (2012).
 - [32] M. Bruderer, K. Franke, S. Ragg, W. Belzig, and D. Obreschkow, *Phys. Rev. A* **85**, 022312 (2012).
 - [33] S. Paganelli, S. Lorenzo, T. J. G. Apollaro, F. Plastina, and G. L. Giorgi, *Phys. Rev. A* **87**, 062309 (2013).
 - [34] N. Y. Yao, Z.-X. Gong, C. R. Laumann, S. D. Bennett, L.-M. Duan, M. D. Lukin, L. Jiang, and A. V. Gorshkov, *Phys. Rev. A* **87**, 022306 (2013).
 - [35] A. Casaccino, S. Lloyd, S. Mancini, and S. Severini, *International Journal of Quantum Information* **7**, 1417 (2007).
 - [36] T. Linneweber, J. Stolze, and G. S. Uhrig, *International Journal of Quantum Information* **10**, 1250029 (2012).
 - [37] S. Lorenzo, T. J. G. Apollaro, A. Sindona, and F. Plastina, *Phys. Rev. A* **87**, 042313 (2013).

- [38] S. Lorenzo, T. J. G. Apollaro, S. Paganelli, G. M. Palma, and F. Plastina, Phys. Rev. A **91**, 042321 (2015).
- [39] A. P. Hines and P. C. E. Stamp, Phys. Rev. A **75**, 062321 (2007).